Available online at www.sciencedirect.com

ScienceDirect

Ceramics International 40 (2014) 4717–4723

CERAMICS INTERNATIONAL

www.elsevier.com/locate/ceramint

A study on partially protonated titanate nanotubes: Enhanced thermal stability and improved photocatalytic activity

Liang Shi[a,b], Lixin Cao[a,b,*], Wei Liu[b], Ge Su[b], Rongjie Gao[b], Yanling Zhao[b]

[a]College of Chemistry and Chemical Engineering, Ocean University of China, Qingdao 266100, PR China
[b]Institute of Materials Science and Engineering, Ocean University of China, Qingdao 266100, PR China

Received 25 July 2013; received in revised form 3 September 2013; accepted 3 September 2013
Available online 11 September 2013

Abstract

Partially protonated titanate nanotubes were prepared via an alkaline hydrothermal process followed by ion-exchange. The protonation level was controlled by varying the amount of HCl. Nanotubes were calcinated within the temperature range of 400–500 °C to investigate the thermal stability of partially protonated titanate nanotubes. X-ray diffraction (XRD), transmission electron microscopy (TEM), inductively coupled plasma spectroscopy (ICP) and N_2 absorption–desorption experiment were employed to characterize the morphology, composition and specific surface area. In addition, photocatalytic activities were also evaluated by photodegradation of methyl orange under the radiation of UV light. The results revealed that 0.5(Na,H)TNTs450, remaining with 0.668 wt% sodium content, retained a tubular structure against calcination, and owned considerable photocatalytic activity with degradation rate near 80%.

Keywords: Titanate nanotubes; Protonation; Thermal stability; Photocatalytic activity

1. Introduction

Since photocatalytic splitting of water on TiO_2 electrodes was discovered by Honda and Fujishima in 1972 [1], titania has been extensively used in several applications such as hydrogen generation [2], sensors [3], solar cell [4] and environmental purification [5,6]. In the last decade many efforts have been focused on developing a novel nanostructure of titania with improved performance in heterogeneous photocatalysis.

Kasuga et al. [7,8] innovated a simple alkaline hydrothermal treatment of crystalline titania particles with concentrated NaOH aqueous solution, to obtain high quality titanium nanotubes with uniform diameter and large specific surface area. The hydrothermal method has the advantages of being simple, cost-effective, and environmental friendly [9] over the templates method and anodic oxidation method, making titanium nanotubes popular among researchers. Unfortunately, the as-prepared nanotubes by this hydrothermal method showed little photocatalytic activity [10], because of the sodium titanate phase formation [11]. Moreover, hydrogen titanate nanotubes with further acid treatment did not possess photocatalytic activity due to low crystallinity [12]. Qamar et al. suggested a key for the above dilemma and found that photocatalytic activity increased when as-prepared nanotubes were washed with diluted acid and then calcined to crystallize [13].

Many researchers have studied the structure of sodium titanate nanotubes together with hydrogen titanate nanotubes. As for as-prepared nanotubes, Na^+ ions are located between titanate layers at a distance larger than that of proton from the nearest oxygen ion, confirming the possibility of protonation via ion-exchange [14]. Studies by Morgado et al. [15] and Sun and Li [16] suggested that sodium cannot be removed completely because of its substantial role in maintaining tubular structure and thermal stability.

Yoshida et al. innovatively proposed partially ion-exchanged titanate nanotubes treated with insufficient acid to clarify the role of sodium ions, neglecting the role of proton in practical use [17]. Lee and colleagues further studied effects of different sodium contents on several properties of nanotubular titanate [18], but still not in detail. In this work, we present partially proton exchanged titanate nanotubes, and then quantitatively investigate the role of sodium ions and proton in

*Corresponding author at: Ocean University of China, College of Chemistry and Chemical Engineering, Qingdao 266100, China. Tel.: +86 532 66781901.
E-mail address: caolixin@ouc.edu.cn (L. Cao).

0272-8842/$ - see front matter © 2013 Published by Elsevier Ltd and Techna Group S.r.l.
http://dx.doi.org/10.1016/j.ceramint.2013.09.013

achieving excellent photocatalytic activity and enhanced thermal stability as well.

2. Experimental

2.1. Synthesis of sodium titanate nanotubes

Sodium titanate nanotubes with uniform diameter and length were synthesized via a hydrothermal process [7,8]. Typically, 1.00 g P25 (70% anatase and 30% rutile, Degussa) were mixed with 50 mL of 10 M NaOH (AR, Sinopharm Chemical Reagent Co., Ltd.) aqueous solution under continuous magnetic stirring for 2 h. Then the mixture was transferred to an 80 mL autoclave and kept at 150 °C for 24 h in an oven. After it was cooled down to ambient temperature, the slurry was centrifuged and washed with distilled water several times until pH of supernatant approached 7.0. Finally, the sediment was dried at 80 °C for 6 h in the oven and ground for further use. For convenience, we represent sodium titanate nanotubes as (Na)TNTs. We assumed that the formula of (Na)TNTs was $Na_2Ti_3O_7$, as supported by Morgado et al. [15].

2.2. Preparation of partially protonated titanate nanotubes

1.00 g (Na)TNTs was dispersed in 40 mL of distilled water and magnetically stirred for 30 min.Then 80 mL of hydrochloric acid solution (AR, Sinopharm Chemical Reagent Co., Ltd.) was poured in the previous white turbid liquid under continuous agitation and the mixture was stirred for 3 h. The concentration of hydrochloric acid solution was denoted by x, which meant that protons were x (x=0, 0.2, 0.5, 1.0, 2.0, 5.0) times the molar amount of Na^+ in the initial (Na)TNTs. In order to purify the samples, the sediment was centrifuged and washed with distilled water for five times. Samples were labeled as x(Na,H)TNTs to make a distinction.

2.3. Heat treatment of samples

In order to investigate thermal stability and photocatalytic activity, samples were calcined at 400, 450, and 500 °C for 90 min at a rate of 3 °C/min. We labeled samples calcined at these temperatures as x(Na,H)TNTs400, x(Na,H)TNTs450 and x(Na,H)TNTs500, correspondingly.

2.4. Characterization

X-ray diffraction (XRD) experiments were performed using a BRUKER D8 ADVANCE X-ray diffractometer fitted with a Cu Kα radiation over the 2θ range from 20° to 70°, and the scanning speed was 5°/min. Morphology of the samples was observed using H-7000 transmission electron microscopy (TEM). The actual sodium content left in the samples was measured by ICAP (6300, Thermal Fisher) followed by dissolving the as-prepared samples in sulfuric acid. Specific surface area was measured on an ST-08A apparatus. An OCRS-I photochemical reactor (Kaifeng Hongxing Machine Electronic Co.) was used to investigate the photocatalytic activity of the samples at ambient temperature. The optical absorption spectra were obtained using an ultraviolet and visible spectrophotometer (Shimadzu UV-2550, Japan).

2.5. Evaluation of the photocatalytic properties

The photocatalytic activity experiments were carried out to degrade 30 mg/L methyl orange (AR, BASFSE) in an OCRS-I photochemical reactor (Kaifeng Hongxing Machine Electronic Co.) at ambient temperature. A 300 W high pressure mercury lamp was used as the light source, which was put in a cylindrical quartz vessel with a circulating water quartz jacket. In a general procedure, 100 mg of sample was added to 60 mL of methyl orange solution. The mixture was stirred in darkness for 30 min to reach adsorption–desorption equilibrium. Then light was turned on, and a total of seven 5 mL aliquots were taken out every 30 min. Suspensions were then centrifuged, and supernatant was collected and analyzed to quantify the concentration of methyl orange by the absorption spectrum [19]. The maximum absorbance of methyl orange molecule A was measured at 465 nm, and the concentration was obtained according to Lambert–Beer's law.

The photocatalytic activity was evaluated from an analysis of the photodegradation of methyl orange, as determined by the following equation [20]:

$$\varphi = (A_0 - A_6)/A_0$$

Here, φ stands for the photodegradation rate of methyl orange, while A_0 and A_6 stand for the absorbance of methyl orange solution before and after the photocatalytic reaction, respectively.

3. Results and discussion

3.1. Morphology and composition analysis

Fig. 1 shows the XRD patterns of the as-prepared sodium titanate and the protonated titanate nanotubes obtained by further treatment with excess amount of hydrochloric acid. It can be seen that the as prepared (Na)TNTs were mainly composed of $Na_2Ti_3O_7$ (JCPDS 31-1329). The peak centered at about 10.5°, which was attributed to interlayer space of layered structure [21], was assigned to the primary peak 001 of $Na_2Ti_3O_7$ [22]. Other peaks at 2θ=24.3°, 28.2° and 48.3° were the characteristic diffractions of tubular $Na_2Ti_3O_7$ [23]. The diffraction pattern of (H)TNTs differed from that of (Na)TNTs where the value at 2θ=24.3° increased but at 28.3° decreased. The discrepancy that emerged after the acid washing process was ascribed to those interlayer sodium ions that were irreversibly exchanged with protons, producing monoclinic $H_2Ti_3O_7$ [24–26] when acid was excessive. Considering that samples obtained by exchanging sodium ions with quantitative protons also lacked crystallization, we performed post-heat treatment and will discuss it in the following section.

As indicated in Fig. 2, the morphologies of both (Na)TNTs and (H)TNTs were multilayered nanotubes, with a length of

several hundred nanometers and diameter of about 10 nm which agreed with previous research [27]. Meanwhile protonated titanate nanotubes changed little in structure and could not be distinguished with sodium titanate nanotubes, and this is consistent with XRD results above. The result demonstrated that tubular samples were obtained before post-heat treatment in protonation with various concentrations.

As different concentrations of hydrochloric acid were employed to trigger the protonation process, the actual sodium contents left in the as-prepared partially titanate nanotubes were characterized by ICP spectra before they were calcinated. As shown in Fig. 3, as-prepared sodium titanate nanotubes possessed an amount of 4.996 wt% sodium, which is smaller than that in previous reports [15,18] owing to sufficient washing with distilled water. With the increase of nominal H^+/Na^+ to 0.5, a substantial decline to 0.668 wt% of sodium content in the samples occurred. However, the remaining sodium content of about 0.05 wt% tended to equilibrium when further protonation proceeded, revealing the fact that sodium cannot be completely removed.

3.2. Effect of post-heat treatment

According to previous reports, titanate nanotubes retained a tubular shape quite well against calcination below 400 °C in air. However, aggregates were generated and the tubular structure collapsed rapidly when the temperature exceeded this value. Therefore the as-prepared samples were treated in the narrow range of 400–500 °C for further investigation.

Fig. 4(a) and (b) shows the TEM images of 0(Na,H)TNTs400 and 5.0(Na,H)TNTs400, respectively, and they present the typical morphologies of all the samples calcinated at 400 °C, which are similar to those of precursors, and this result agrees with that of Nosaka et al. [28]. However, all samples collapsed in the range of our protonation degree at the calcination temperature of 500 °C, as shown in Fig. 4(c) and (d), which is consistent with the study by Sreekantan and Wei [29].

Thus the treating temperature was slightly increased by 50 °C, a series of (Na,H)TNTs450 samples were obtained, and their TEM images are shown in Fig. 5. Due to high sodium content [18], as we measured in Fig. 3, samples 0(Na,H)TNTs450 and 0.2(Na,H)TNTs450 retained fine tubular shape and dispersity. In Fig. 5(c), 0.5(Na,H)TNTs retained an almost tubular structure but shortened in length. Though intralayer dehydration had begun with the increase of protons, there was still 0.668 wt% of sodium ions to retain the tubular structure. Nanotubes were seldom found in the view of 1.0(Na,H)TNTs450 image because most sodium ions were removed under a high proton concentration, and only 0.192 wt% sodium cannot retain the tubular structure of protonated titanate. With

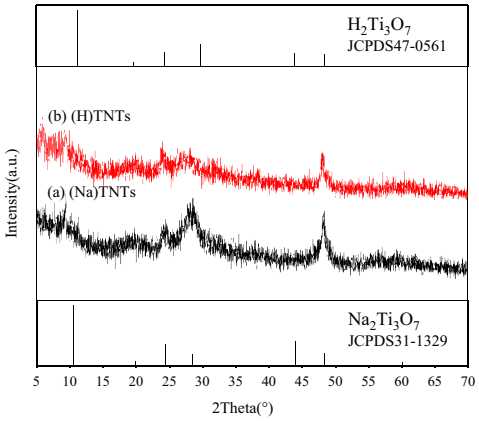

Fig. 1. XRD patterns of (a) as-prepared sodium titanate nanotubes and (b) protonated titanate nanotubes.

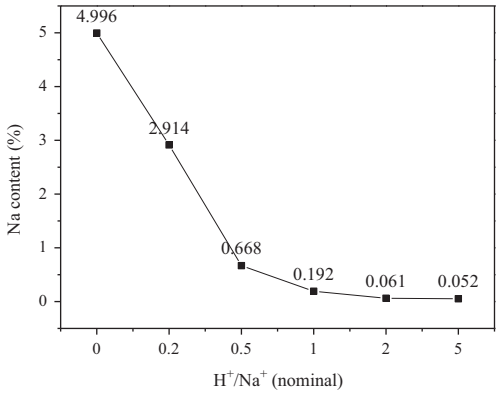

Fig. 3. Actual sodium content in as-prepared sodium titanate nanotubes and partially protonated titanate nanotubes.

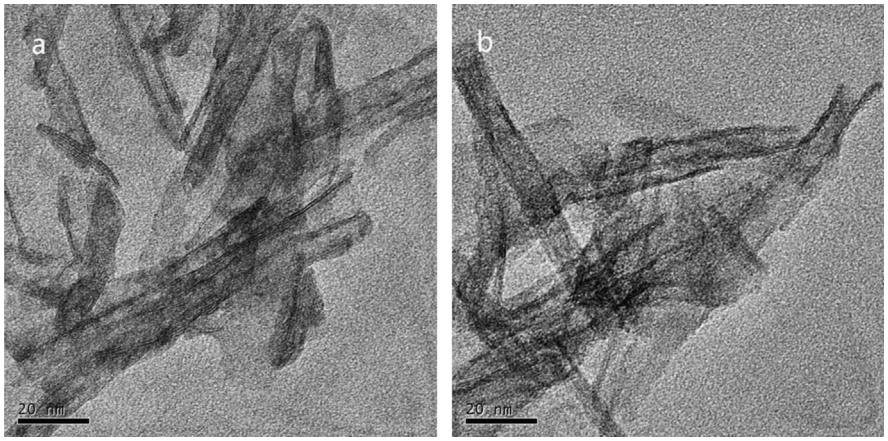

Fig. 2. TEM images of (a) as-prepared sodium titanate nanotubes and (b) protonated titanate nanotubes.

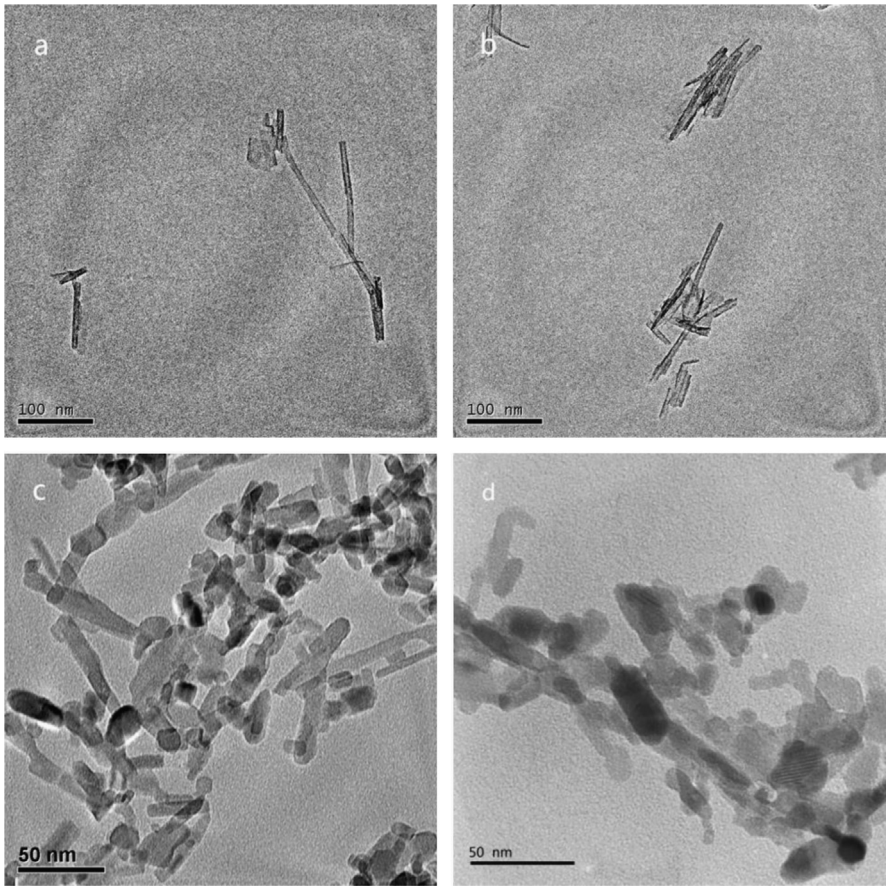

Fig. 4. TEM images of calcinated nanotubes: (a) 0(Na,H)TNTs400, (b) 5.0(Na,H)TNTs400, (c) 0(Na,H)TNTs500 and (d) 5.0(Na,H)TNTs500.

the further increase of proton percentage, samples 2.0(Na,H) TNTs and 5.0(Na,H)TNTs collapsed into nanostripes and nanorods, respectively, which was caused by different pressures in the inner and outer surfaces of nanotubes [30,31]. These results reflected that the intralayer sodium content was about 0.668 wt% of the samples, which was critical for structural maintenance under 450 °C calcination.

In order to investigate the transformation of composition and structure as the H:Na ratio increases, X-ray diffraction experiment was performed for the samples. Fig. 6 shows the XRD patterns of the series of samples calcinated at 450 °C. 0(Na,H) TNTs450 revealed a distinctive pattern among the samples without anatase, demonstrating a typical $Na_2Ti_3O_7$ (JCPDS 31-1329) composition as that of precursor except for better crystallization. 0.2(Na,H)TNTs450 began to show a typical anatase phase (JCPDS 21-1272) attributed to protonation. However, the crystallization was far from complete because of low protonated degree and a broad peak of $Na_2Ti_3O_7$ can be found at about 10.5° by careful observation. Fig. 6(c)–(f) shows a group of similar patterns except tiny differences in crystallinity, reflecting fine anatase composition in the major phase. A weak peak centered at about 12.5° was found for the $Na_2Ti_4O_9$ mixture (JCPDS 33-1294 and JCPDS 37-0951), and this observation is consistent with the conclusion that sodium ions cannot be removed completely as measured above because at this structural composition the intralayer sodium ions did not participate in the protonation process.

Fig. 6(g) and (h) shows XRD patterns of 5.0(Na,H) TNTs400 and 5.0(Na,H)TNTs500, and a series of samples with given protonation were clearly compared together with that of Fig. 6(f). As a result of high protonation degree derived from the identical precursor, the content and crystallinity of anatase were determined by calcination. As shown in Fig. 6(f)–(h), calcination at 400 °C led to a much poorer crystallinity of anatase.

3.3. Photocatalytic activity

Organic dye methyl orange molecule was employed as a probe to evaluate the photocatalytic activities of all the calcinated samples. The initial concentration of methyl orange was 30 mg/L, higher than the common amount of 20 mg/L in previous literatures [32,33], to avoid deviation caused by prematurely complete degradation. Fig. 7 lists the final degradation rate of all the samples synthesized and post-processed. From Fig. 7 we reached descriptive results that the degradation rate became larger as the protonation degree increased. This can be easily explained in Fig. 6; a large amount of anatase was generated with increase of proton percentage, because of structural similarity between anatase and protonated titanate [34]. Calcinated 0(Na,H)TNTs and 0.2(Na,H)TNTs exhibited poor photocatalytic activity because of low anatase content and crystallinity, which contradicted with the work of Morgado et al. [15], where no photocatalytic

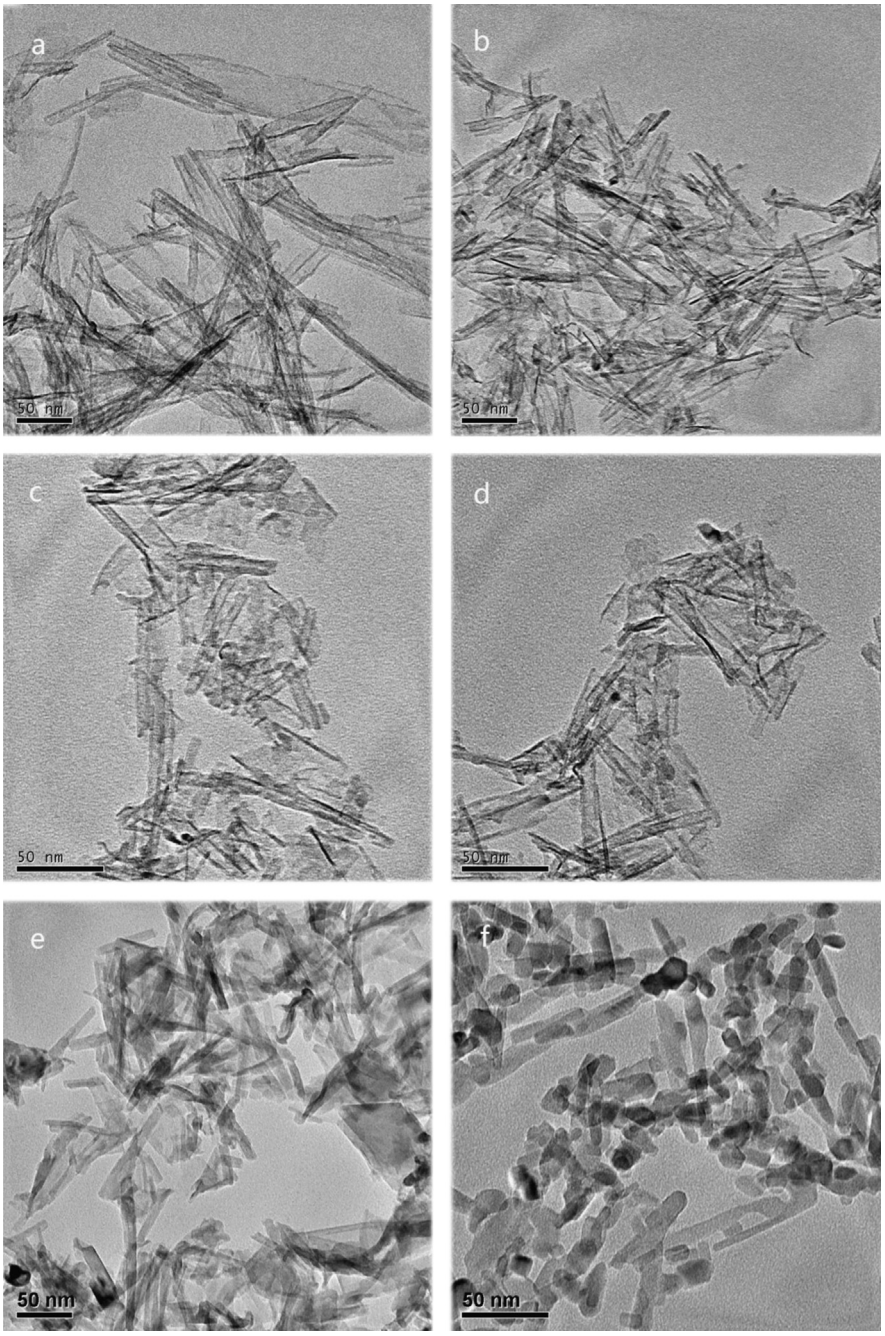

Fig. 5. TEM images of x(Na,H)TNTs450: (a) $x=0$, (b) $x=0.2$, (c) $x=0.5$, (d) $x=1.0$, (e) $x=2.0$, and (f) $x=5.0$.

activity was found for samples with protonation degree below 0.5. Samples protonated above 0.5 showed slow growth of final degradation rate due to similar crystallinity revealed in Fig. 6

Fig. 7 also shows that samples calcinated at higher temperature owned better photocatalytic activities, which is in accordance with previous research works [30,31], owing to better crystallinity of anatase with the same protonation degree. However, 0.5(Na,H)TNTs were proven to be distinctive since 0.5(Na,H)TNTs450 exceeded 0.5(Na,H)TNTs500 in photocatalytic activity.

In order to make the discrepancy clear and quantified, the rate constant for the photocatalytic reaction was calculated from linear fitting curves shown in Fig. 8, since photocatalytic degradation followed first-order kinetics and the slope of linear regression represents the apparent reaction rate constant k. As shown in Fig. 8, the photocatalytic reaction rate constant of 0.5(Na,H)TNTs450 was as high as 0.00763 min^{-1}, which evidently exceeded that of 0.5 (Na,H)TNTs400 and 0.5(Na,H)TNTs500. The large photocatalytic activity of 0.5(Na,H)TNTs450 can be attributed to collaboration of good crystallinity and tubular structure, which led to a unique formation of anatase nanotubes with a high specific surface area.

Table 1 lists values of specific surface area for all samples, obtained by the N_2 absorption–desorption experiment. All precursors possessed large specific surface area over 300 m^2/g, owing to their tubular morphologies as discussed before. A slight decrease in specific surface area was found for samples

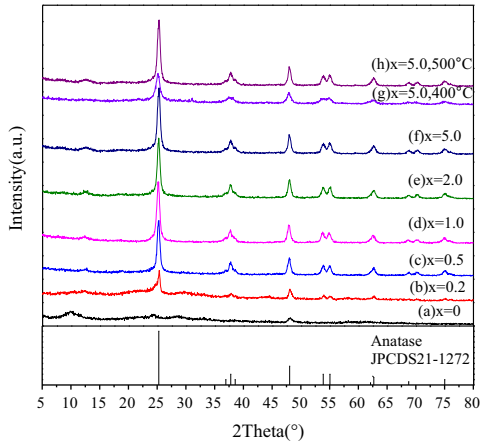

Fig. 6. XRD patterns of x(Na,H)TNTs450: (a) $x=0$, (b) $x=0.2$, (c) $x=0.5$, (d) $x=1.0$, (e) $x=2.0$ and (f) $x=5.0$, and 5.0(Na,H)TNTs at (g) 400 °C and (h) 500 °C.

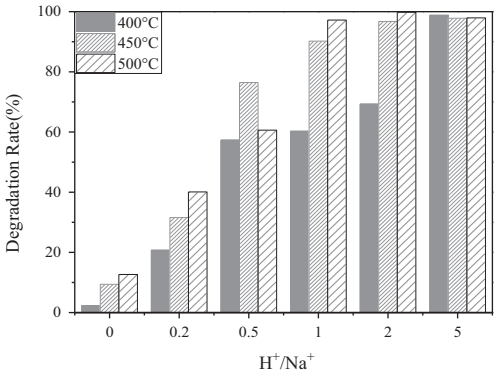

Fig. 7. Graph of photocatalytic degradation rate of all the calcinated samples.

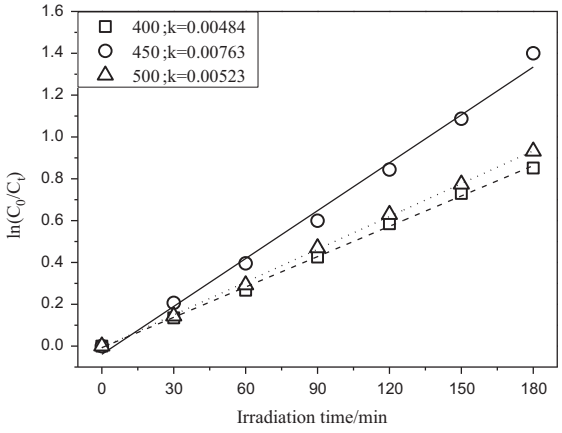

Fig. 8. Linear fitting plots of 0.5(Na,H)TNTs calcinated at different temperatures: (□) 400 °C, (○) 450 °C and (Δ) 500 °C.

calcinated at 400 °C, and aggregation caused by calcination was responsible for this change. For samples calcinated at 450 °C, sodium ions played an important role in maintaining a tubular structure against dehydration caused by heat treatment; thus nanotubes still appeared as revealed in Fig. 5(a)–(c) though specific surface area reduced by half. From the critical point of 0.5(Na,H)TNTs450, further

Table 1
Specific surface area values of all the samples.

x(Na,H)TNTs	Specific surface area (m^2/g)			
	Precursors	400 °C	450 °C	500 °C
0	368	285	144	67
0.2	342	298	132	63
0.5	334	287	129	60
1.0	327	287	80	54
2.0	329	256	80	50
5.0	330	278	82	56

protonation or temperature elevation made specific surface area to drop below 80, as Fig. 5(d)–(f) indicated collapse of tubular structure. For 0.5(Na,H)TNTs450, good crystallinity as indicated by Fig. 6(c) and twice the specific surface area as that of 0.5(Na,H)TNTs500 contributed to the best photocatalytic activity among samples with the same proton content.

As indicated in Fig. 7, the similar degradation rate of 5.0 (Na,H)TNTs also testified the significance that specific surface area played in photocatalytic activity. The crystallinity of 5.0 (Na,H)TNTs calcinated at 400 °C was evidently poorer than that of samples calcinated at higher temperature as shown in Fig. 6(f)–(h), so the high photocatalytic activity was largely attributed to the large specific surface area measured in Table 1 which was derived from a tubular structure radically as shown in Fig. 4(b).

4. Conclusion

Partially protonated titanate nanotubes were initially fabricated via a quantified acid washing procedure after the hydrothermal synthesis. Post treatments were carried out to investigate the thermal stability of partially protonated titanate nanotubes, and the morphology, composition and specific surface area were characterized. A photocatalytic degradation experiment was performed to evaluate the photocatalytic activity of all the samples. As a result, 0.5(Na,H)TNTs remained with 0.668 wt% of sodium content in the intralayer, which was significant for maintaining a tubular structure, and revealing optimum synergy of thermal stability and photocatalytic activity in 0.5(Na,H)TNTs450. Although there was room for an increase of the photocatalytic activity, 0.5(Na,H) TNTs450 had already reached nearly 80% degradation, close to the maximum of calcinated totally protonated titanate.

Acknowledgments

The authors are very grateful to the National Science Foundation of China (NSFC 51172218) for financial support through Qingdao Science and Technology Development Project (12-1-4-1-(2)-jch) and Promotive Research Fund for Young and Middle-Aged Scientists of Shandong Province (BS2010CL049).

References

[1] A. Fujishima, K. Honda, Nature 238 (1972) 37.
[2] Z. Zhang, M.F. Hossain, T. Takahashi, International Journal of Hydrogen Energy 35 (2010) 8528.
[3] E. Şennik, Z. Çolak, N. Kılınç, Z.Z. Öztürk, International Journal of Hydrogen Energy 35 (2010) 4420.
[4] P. Sudhagar, J.H. Jung, S. Park, R. Sathyamoorthy, H. Ahn, Y.S. Kang, Electrochimica Acta 55 (2009) 113.
[5] M.R. Hoffmann, S.T. Martin, W. Choi, D.W. Bahnemann, Chemical Reviews 95 (1995) 69.
[6] A. Fujishima, T.N. Rao, D.A. Tryk, Journal of Photochemistry and Photobiology C: Photochemistry Reviews 1 (2000) 1.
[7] T. Kasuga, M. Hiramatsu, A. Hoson, T. Sekino, K. Niihara, Langmuir 14 (1998) 3160.
[8] M.H.T. Kasuga, A. Hoson, T. Sekino, K. Niihara, Advanced Materials 11 (1999) 1307.
[9] A. Thorne, A. Kruth, D. Tunstall, J.T. Irvine, W. Zhou, Journal of Physical Chemistry B 109 (2005) 5439.
[10] N. Bouazza, M. Ouzzine, M.A. Lillo-Ródenas, D. Eder, A. Linares-Solano, Applied Catalysis B: Environmental 92 (2009) 377.
[11] J. Yang, Z. Jin, X. Wang, W. Li, J. Zhang, S. Zhang, X. Guo, Z. Zhang, Dalton Transactions (2003) 3898.
[12] K. Nishijima, Y. Fujisawa, N. Murakami, T. Tsubota, T. Ohno, Applied Catalysis B: Environmental 84 (2008) 584.
[13] M. Qamara, C.R. Yoon, H.J. Oh, N.H. Lee, K. Park, D.H. Kim, K.S. Lee, W.J. Lee, S.J. Kim, Catalysis Today 131 (2008) 3.
[14] L. Miao, S. Tanemura, R. Huang, C.Y. Liu, C.M. Huang, G. Xu, ACS Applied Materials & Interfaces 2 (2010) 2355.
[15] E. Morgado, M.A.S. de Abreu, O.R.C. Pravia, B.A. Marinkovic, P.M. Jardim, F.C. Rizzo, A.S. Araújo, Solid State Sciences 8 (2006) 888.
[16] X. Sun, Y. Li, Chemistry 9 (2003) 2229.
[17] R. Yoshida, Y. Suzuki, S. Yoshikawa, Materials Chemistry and Physics 91 (2005) 409.
[18] C.K. Lee, C.C. Wang, M.D. Lyu, L.C. Juang, S.S. Liu, S.H. Hung, Journal of Colloid and Interface Science 316 (2007) 562.
[19] C.J.G. Cornu, A.J. Colussi, M.R. Hoffmann, Journal of Physical Chemistry B 107 (2003) 3156.
[20] C. Lv, Y. Zhou, H. Li, M. Dang, C. Guo, Y. Ou, B. Xiao, Applied Surface Science 257 (2011) 5104.
[21] C.K. Lee, K.S. Lin, C.F. Wu, M.D. Lyu, C.C. Lo, Journal of Hazardous Materials 150 (2008) 494.
[22] Y. Zhang, W. Fu, H. Yang, M. Li, Y. Li, W. Zhao, P. Sun, M. Yuan, D. Ma, B. Liu, G. Zou, Sensors and Actuators B: Chemical 135 (2008) 317.
[23] M. Wei, Y. Konishi, H. Zhou, H. Sugihara, H. Arakawa, Solid State Communications 133 (2005) 493.
[24] A. Riss, T. Berger, H. Grothe, J. Bernardi, O. Diwald, E. Knozinger, Nano Letters 7 (2007) 433.
[25] D. Wu, J. Liu, X. Zhao, A. Li, Y. Chen, N. Ming, Chemistry of Materials 18 (2006) 547.
[26] D.V. Bavykin, A.A. Lapkin, P.K. Plucinski, J.M. Friedrich, F.C. Walsh, Journal of Physical Chemistry B 109 (2005) 19422.
[27] M. Xiao, L. Wang, X. Huang, Y. Wu, Z. Dang, Journal of Alloys and Compounds 470 (2009) 486.
[28] J. Suetake, A.Y. Nosaka, K. Hodouchi, H. Matsubara, Y. Nosaka, Journal of Physical Chemistry C 112 (2008) 18474.
[29] S. Sreekantan, L.C. Wei, Journal of Alloys and Compounds 490 (2010) 436.
[30] J.C. Xu, M. Lu, X.Y. Guo, H.L. Li, Journal of Molecular Catalysis A: Chemical 226 (2005) 123.
[31] J. Yu, H. Yu, B. Cheng, C. Trapalis, Journal of Molecular Catalysis A: Chemical 249 (2006) 135.
[32] M. Huang, C. Xu, Z. Wu, Y. Huang, J. Lin, J. Wu, Dyes and Pigments 77 (2008) 327.
[33] J.C. Xu, Y.-L. Shi, J.-E. Huang, B. Wang, H.L. Li, Journal of Molecular Catalysis A: Chemical 219 (2004) 351.
[34] T. Kubo, A. Nakahira, Journal of Physical Chemistry C 112 (2008) 1658.